

## Spectroscopic study of process of carbon ablation from a graphite surface under shock wave influence

© M.A. Kotov<sup>1,2</sup>, P.V. Kozlov<sup>1</sup>, V.Yu. Levashov<sup>1</sup>, G.Ya. Gerasimov<sup>1</sup>, N.G. Bykova<sup>1</sup>, I.E. Zabelinskij<sup>1</sup>

<sup>1</sup> Institute of Mechanics of Lomonosov Moscow State University, Moscow, Russia

<sup>2</sup> Ishlinsky Institute for Problems in Mechanics, Russian Academy of Sciences, Moscow, Russia

E-mail: kotov@ipmnet.ru

Received April 15, 2024

Revised July 9, 2024

Accepted October 30, 2024

The spectral characteristics of the products of graphite surface ablation behind a reflected shock wave in air were studied in the wavelength range from 400 to 1100 nm. The experiments were carried out on a single-diaphragm shock tube. It has been shown that the emission spectrum of ablation products is close to the emission spectrum of an absolutely black body. Additional experiments on the reflection of a shock wave from a quartz surface allow us to conclude that the detected electromagnetic flux is associated with the emission of solid carbon microparticles formed in the air near the graphite surface as a result of the impact of a shock wave on it.

**Keywords:** shock wave, radiation spectrum, ablation, carbon microparticles.

DOI: 10.61011/TPL.2024.12.60341.6247k

The movement of a descent vehicle through the Earth's atmosphere is associated with large thermal loads on its surface. Therefore, the design of reliable thermal protection systems is relevant to the development of advanced space hardware. A considerable number of experimental and theoretical studies into convective and radiative heat flows behind a reflected shock wave, which affect a descent vehicle, have already been published [1–3]. Simulation of the response of the surface protective layer of the vehicle to thermal loads is crucial for promotion of flight safety [4].

Carbon-based composite materials are commonly used to construct thermal protection systems. Various experimental setups are used to study the ablation properties of such materials. First off, these are continuous-action setups, such as a plasma wind tunnel [5] and an electric arc facility [6], which allow one to examine the material response to the thermochemical influence of a low-temperature plasma flow. In the case of pulsed loads, laser installations [7], which make it possible to estimate the concentrations of various carbon-containing components in the products of laser ablation of the graphite sample surface, and shock tubes [8], which have the capacity to reproduce the supersonic flow past a tested model after the passage of a shock wave, are used. The current state of experimental and theoretical research into ablation of the thermal protection layer of a descent vehicle moving through the Earth's atmosphere has been discussed recently in [9].

In the present study, ablation processes proceeding in air near a graphite surface after a strong shock wave is reflected from it are subjected to spectroscopic examination. Experiments were carried out in a single-diaphragm shock tube that is a part of the experimental complex at the Institute of Mechanics of Moscow State University. Its internal diameter is 57 mm, and the length of high and low pressure chambers is 1.0 and 3.7 m, respectively. A copper

diaphragm with calibrated notches is mounted between the chambers. The setup was described in detail in [10].

The measurement system of the setup, which is shown schematically in Fig. 1, features two recording channels. The first one uses a PMT-100 photomultiplier and a MC-300 monochromator to record the time profile of emission. The monochromator grating was operated in the „zero-order“ mode as a mirror reflecting radiation within the spectral range of 200–2500 nm. The photomultiplier tube has a spectral sensitivity region of 170–850 nm. The second measuring channel records the time-integrated emission intensity within the VIS/IR spectral range ( $\lambda = 400–1100$  nm) with a Hamamatsu S11156 linear CCD sensor, which is installed at the output of a Horiba 1824 spectrograph. The photosensitivity of this sensor is adjusted depending on the emission wavelength. The observing line passes at a distance of 0.5 mm from the sample surface. The bulk of emission (approximately 90%) is recorded from a cylinder with a diameter of 1 mm and a length of 57 mm. The edge of pressure sensor  $D$  (PCB 113B24) is adjacent to the sample. The process time is measured from the moment of formation of a reflected shock wave (RSW). Shock wave velocity  $V_{SW}$  is determined using pressure sensors located on the side surface of the shock tube.

The spectral characteristics of products of ablation of the graphite surface behind a reflected shock wave are presented in Fig. 2. These data were obtained at initial pressure  $P_1 = 6118$  Pa in the low-pressure chamber and shock wave velocity  $V_{SW} = 1.58$  km/s. High-density 3OPG graphite with an enhanced structure was the test sample. The gas temperature behind a reflected shock wave was calculated to be  $T = 2500$  K based on the initial parameters of the shock process in GASEQ [11]. It can be seen from Fig. 2, *a* that the time dependence of pressure has two characteristic plateaus. The first plateau is associated with

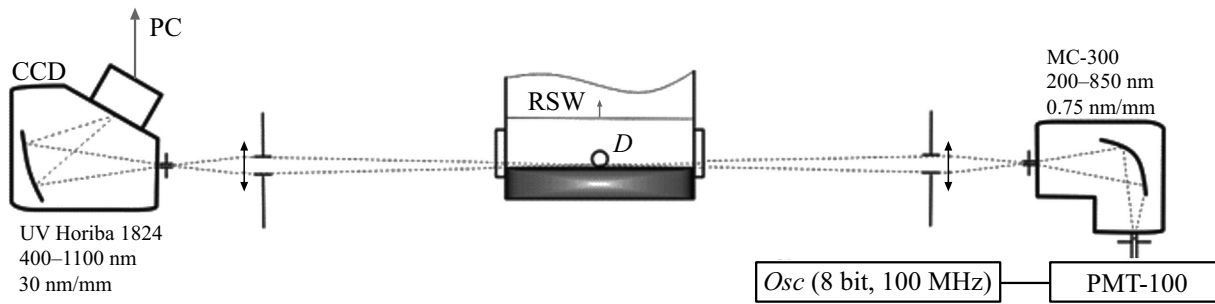


**Figure 1.** Schematic diagram of the shock tube measurement system. CCD UV Horiba 1824 — spectrograph, PC — personal computer, RSW — reflected shock wave,  $D$  — pressure sensor, MC-300 — monochromator, PMT-100 — photomultiplier tube, and *Osc* (8 bit, 100 MHz) — oscilloscope.

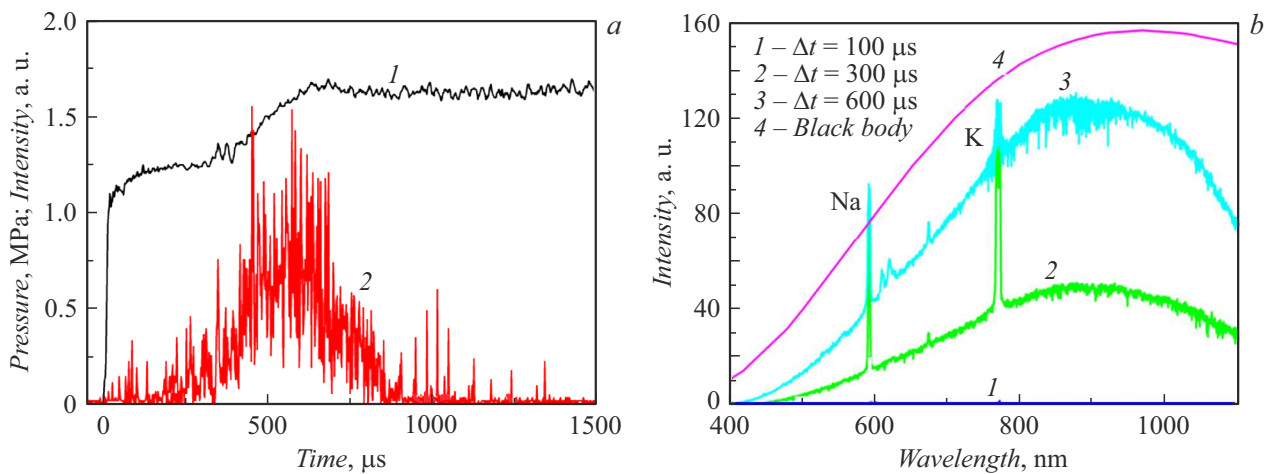


**Figure 2.** Evolution of gas pressure behind a reflected shock wave ( $I$ ) and emission intensity within the wavelength range of 200–850 nm ( $2$ ) (a) and emission spectrum (b) of the products of ablation of a graphite surface at  $P_1 = 6118$  Pa and  $V_{SW} = 1.58$  km/s. The curve for  $\Delta t = 100 \mu\text{s}$  is almost indistinguishable from the abscissa axis.

a pressure jump when a shock wave is reflected from the graphite surface. The second plateau indicates the arrival of a rereflected shock wave from the contact surface between the test and driving gases. The initial stage of the process under study (between the moment of reflection of a shock wave from the graphite surface and the onset of emission;  $t \leq 200 \mu\text{s}$ ) is an induction period, wherein the emission intensity of products of ablation of the graphite surface is virtually equal to zero. As the process evolves further, the emission intensity increases sharply, reaches a maximum in the interval from 400 to  $700 \mu\text{s}$ , and decreases.

The time-integrated emission intensity (Fig. 2, b) determined at different time intervals  $\Delta t$  from the start of the process verifies the presence of an induction period and a subsequent rapid increase in emission intensity. Quantity  $\Delta t$  is understood here as the time of integration of the emission signal from the start of the process (the moment of reflection of a shock wave from the graphite surface) to point  $t$ . Figure 2, b shows the blackbody spectrum calculated at  $T = 2500$  K. A comparison of the presented spectrograms reveals that the emission spectrum of ablation products of the graphite surface is close to the blackbody

spectrum. This suggests that emission recorded within this spectral range is likely to be produced by solid carbon microparticles that broke off from the graphite surface when it was exposed to a shock wave. In this case, the induction period may be understood as the time interval of heating of cool microparticles to the temperature of shock-heated gas. It should be noted that the emission spectrum shown in Fig. 2, b is a time-averaged one. Therefore, one cannot state with certainty that it is dominated by emission corresponding to the maximum temperature of ablation products, which matches the temperature of shock-heated gas. Consequently, the comparison of the emission spectrum of ablation products with the blackbody spectrum at a certain temperature is not altogether correct.

As the shock wave intensity increases, the radiation power increases sharply. Specifically, with an increase in  $V_{SW}$  from 1.4 km/s at  $P_1 = 6250$  Pa to 2.2 km/s at  $P_1 = 10000$  Pa, the time-integrated emission intensity increases by approximately an order of magnitude. This may be associated not only with the growth of gas temperature behind a reflected shock wave, but also with an increase in the number of carbon microparticles formed. Alkali

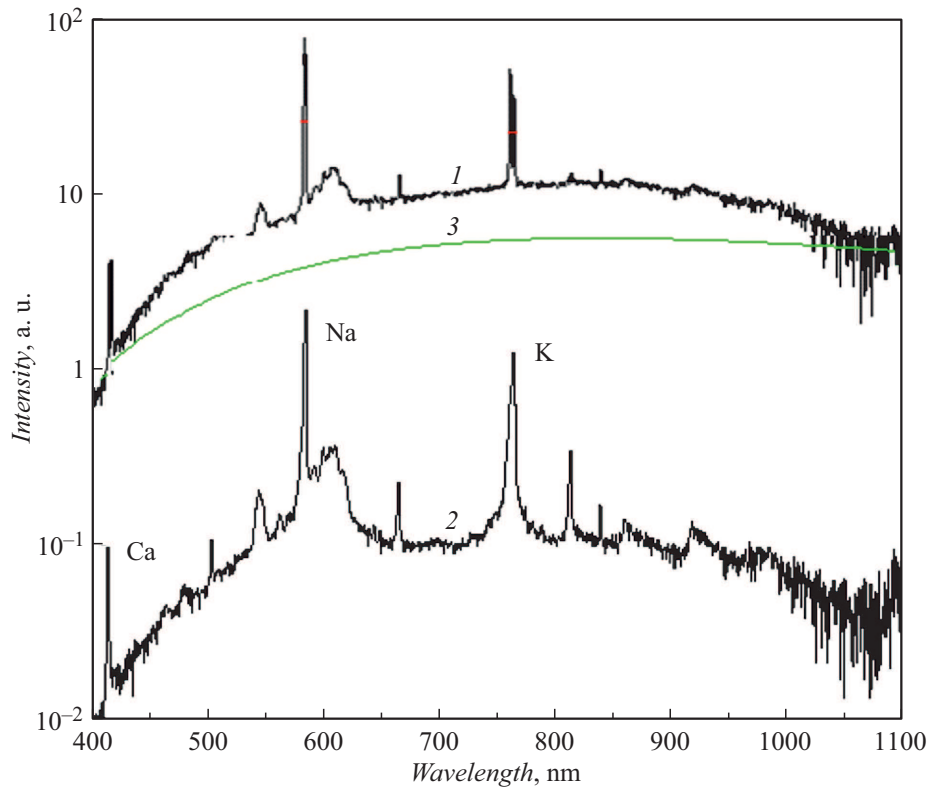


**Figure 3.** Time-integrated intensity of emission of ablation products of graphite (1) and quartz (2) surfaces at  $P_1 = 1000$  Pa and  $V_{SW} = 2.2$  km/s. 3 — Blackbody spectrum calculated at  $T = 3600$  K.

metal lines emerging in the emission spectrum are likely to be attributable to luminescence of quartz glass of the observation windows under the influence of hard radiation from the vacuum ultraviolet region, which is produced behind the front of a reflected shock wave.

A series of experiments on reflection of a shock wave from a quartz surface were conducted in order to ascertain the fact that emission is produced by solid carbon microparticles released into the ambient air from a graphite surface subjected to a pulsed impact of a shock wave. Figure 3 presents a comparison of emission spectra obtained at  $P_1 = 1000$  Pa and  $V_{SW} = 2.2$  km/s within  $\Delta t = 400 \mu\text{s}$  after the reflection of a shock wave from graphite and quartz surfaces. In the case under consideration, the gas temperature behind the reflected wave is 3600 K. Curve 3 represents the blackbody spectrum calculated at  $T = 3600$  K. It can be seen that the recorded time-integrated emission intensity in the case of reflection of a shock wave from a quartz surface is two orders of magnitude lower.

Estimates relying on the solution of the heat transfer equation reveal that the graphite surface temperature increases only by a few tens of degrees within the observation interval due to heat transfer from shock-heated air. A surface temperature this low makes various physical and chemical processes, including sublimation, aspects of heterogeneous systems, and condensation of gaseous ablation products, infeasible. In view of this, it is fair to assume

that the primary mechanism of formation of carbon microparticles near the sample under study is their spallation from the graphite surface under pulsed mechanical loads at the moment of reflection of an incident shock wave from the surface. Only a few studies into this mechanism have been published to date (see, e.g., [12–14]). Therefore, the results obtained here constitute a significant contribution to our understanding of ablation processes proceeding in the vicinity of a graphite surface exposed to a shock wave. It should be noted that an additional examination of the surface of graphite samples before and after the experiments is needed to state with certainty that the indicated mechanism of formation of graphite microparticles is dominant.

Thus, the results of spectroscopic studies revealed that carbon microparticles form near the surface of a graphite sample when a strong shock wave is reflected from it. The emission spectrum of these particles is close to a blackbody one. Theoretical estimates suggest that the primary mechanism of formation of microparticles is their spallation from the graphite surface.

## Funding

This study was carried out under state assignment of the Ministry of Science and Higher Education of the Russian Federation „Experimental and Theoretical Study of Kinetic

Processes in Gases“ (state registration number AAAA-A19-119012990112-4).

### Conflict of interest

The authors declare that they have no conflict of interest.

### References

- [1] B.A. Cruden, A.M. Brandis, J. Thermophys. Heat Transfer, **34** (1), 154 (2020). DOI: 10.2514/1.T5735
- [2] Y. Zhao, H. Huang, Acta Astron., **169**, 84 (2020). DOI: 10.1016/j.actaastro.2020.01.002
- [3] P.V. Kozlov, N.G. Bykova, G.Ya. Gerasimov, V.Yu. Levashov, M.A. Kotov, I.E. Zabelinsky, Acta Astron., **214**, 303 (2024). DOI: 10.1016/j.actaastro.2023.10.033
- [4] V.T. Le, N.S. Ha, N.S. Goo, Composites B, **226**, 109301 (2021). DOI: 10.1016/j.compositesb.2021.109301
- [5] A. Fagnani, B. Helber, A. Hubin, O. Chazot, Meas. Sci. Technol., **34** (7), 075401 (2023). DOI: 10.1088/1361-6501/acc67c
- [6] F. Grigat, S. Loehle, F. Zander, S. Fasoulas, in *AIAA Scitech 2020 Forum* (Orlando, FL, 2020), AIAA paper 2020-1706. DOI: 10.2514/6.2020-1706
- [7] G. Radhakrishnan, P.M. Adams, L.S. Bernstein, J. Appl. Phys., **134** (1), 013303 (2023). DOI: 10.1063/5.0153331
- [8] S.W. Lewis, R.G. Morgan, T.J. McIntyre, J. Spacecraft Rockets, **53** (5), 887 (2016). DOI: 10.2514/1.A33267
- [9] N.N. Mansour, F. Panerai, J. Lachaud, T. Magin, Annu. Rev. Fluid Mech., **56**, 549 (2024). DOI: 10.1146/annurev-fluid-030322-010557
- [10] A.M. Tereza, P.V. Kozlov, G.Ya. Gerasimov, V.Yu. Levashov, I.E. Zabelinsky, N.G. Bykova, Acta Astron., **204**, 705 (2023). DOI: 10.1016/j.actaastro.2021.11.001
- [11] *A chemical equilibrium program for Windows* [Electronic source]. <http://www.gaseq.co.uk/>
- [12] C. Park, G.A. Raiche II, D.M. Driver, J. Thermophys. Heat Transfer, **18** (4), 519 (2004). DOI: 10.2514/1.8098
- [13] A. Martin, C.C. Bailey, F. Panerai, R.S.C. Davuluri, H. Zhang, A.R. Vazsonyi, Z.S. Lippay, N.N. Mansour, J.A. Inman, B.F. Bathel, S.C. Splinter, P.M. Danchy, CEAS Space J., **8** (4), 229 (2016). DOI: 10.1007/s12567-016-0118-4
- [14] K.J. Price, J.M. Hardy, C.G. Borchetta, S.C.C. Bailey, A. Martin, in *AIAA Aviation 2020 Forum* (Virtual event, 2020), AIAA paper 2020-3279. DOI: 10.2514/6.2020-3279

*Translated by D.Safin*